Mechanics of Advanced Composite Structures 10 (2023) 419 – 436

Semnan University

Mechanics of Advanced Composite Structures

journal homepage: http://MACS.journals.semnan.ac.ir

Free Vibration and Buckling Analyses of Nanobeam Embedded in Pasternak Foundation

Y. Kumar [a*], I. Ali [b]

[a] *Department of Mathematics, Government Girls Degree College, Behat-247121, Uttar Pradesh, India*
[b] *Department of Mathematics, Government P.G. College, Gopeshwar-246401, Uttarakhand, India*

KEYWORDS

Free vibration;
Buckling;
Nonlocal;
Nanobeam;
Euler-Bernoulli beam theory;
Pasternak foundation;
PDQM;
HDQM.

ABSTRACT

In this paper, free transverse vibration and buckling analyses of a nanobeam are presented by coupling the Euler-Bernoulli beam (EBT) theory and Eringen's nonlocal elasticity theory. The nanobeam is embedded in the Pasternak foundation. Hamilton's energy principle is used to derive governing differential equations. The Lagrange polynomial-based differential quadrature method (PDQM) and a harmonic differential quadrature method (HDQM) are used to convert the governing differential equation and boundary conditions into a set of linear algebraic equations. The first three frequencies and the lowest critical buckling loads for clamped-clamped, clamped-simply supported, and simply supported-simply supported boundary conditions are obtained by implementing the bisection method through a computer program written in C++. The impacts of nonlocal Eringen's parameter (scaling effect parameter), boundary conditions, axial force, and elastic foundation moduli on frequencies are examined. The effects of nonlocal Eringen's parameter, boundary conditions, and elastic foundation moduli on critical buckling load are also studied. A convergence study of both versions of DQM is conducted to validate the present analysis. A comparison of frequencies and critical buckling loads with those available in the literature is presented.

1. Introduction

After the invention of carbon nanotubes (Iijima [1]), small-scale structures and devices have been developed due to advancements in nanotechnology and nanoscience. Nanobeams and carbon nanotubes are used in micro-electromechanical systems (MEMS), nano-electromechanical systems (NEMS), microactuators, transistors and microsensors, etc. Due to the wide applications of nanotechnology and nanoscience in modern science and technology, researchers have carried out extensive research on nanomaterials. Nanobeams are used in cancer treatment. To propose new designs, an analysis of the mechanical behavior of nanobeams becomes necessary. This problem can be solved by atomistic mechanics (Baughman et al. [2]), hybrid atomistic-continuum mechanics (Wang et al. [3]), and continuum mechanics approach. The first two approaches are computationally expensive and time-consuming. Therefore, the continuum mechanics approach has been used by researchers to model nano-systems as rods, beams, plates, and shells. In this approach, crystal material architecture is replaced by a continuous medium having homogeneous properties. This continuous medium can predict the overall response of the nanomaterial. Hence, new constitutive laws are required to study the nanoscale size effects. Up to a certain size, classical theories can be used to study the behavior of structures. Eringen's nonlocal elasticity theory [4-7] has been proposed to incorporate the nanoscale effect. The work related to free vibration and buckling of a nanobeam has been reported in the literature as follows: Lu et al. [8] derived frequency equations and mode functions of a nonlocal Euler-Bernoulli beam. Xu [9] investigated free transverse vibration of nano-to-micron scale beams using the integral

* Corresponding author. Tel.: +91-9997125309
E-mail address: yaju_saini@yahoo.com

DOI: 10.22075/macs.2023.29904.1477
Received 2023-02-13; Received in revised form 2023-05-09; Accepted 2023-06-08.

equation approach. Wang et al. [10] solved the free vibration problem of micro/nano beams analytically for different combinations of classical boundary conditions. Challamel and Wang [11] presented a small length scale effect for a nonlocal cantilever beam. Murmu and Pradhan [12] used the differential quadrature method to obtain the natural frequencies of a nonuniform cantilever nanobeam. Roque et al. [13] studied the bending, buckling, and free vibration of Timoshenko nanobeams using the meshless method. Mohammadi and Ghannadpour [14] used Chebyshev polynomials in the Rayleigh-Ritz method to study the free vibration of Timoshenko nanobeams. Li et al. [15] investigated the dynamics and stability of transverse vibration of nonlocal nanobeams under variable axial load. Vibration analysis of Euler-Bernoulli nanobeams has been presented by Eltaher et al. [16] using the finite element method. Behra and Chakraverty [17] used orthogonal polynomials in the Rayleigh-Ritz method to obtain frequency parameters and mode shapes of Euler and Timoshenko nanobeams. Rahmani and Pedram [18] presented a closed-form solution for the vibration behavior of functionally graded Timoshenko nanobeams. In another paper, Behra and Chakraverty [19] applied the differential quadrature method to study the free vibration of nanobeams based on various nonlocal theories. Ebrahimi and Salari [20] studied free flexural vibration of functionally graded nanobeams using the differential transform method. Ebrahimi et al. [21] investigated the vibrational characteristics of functionally graded nanobeams using the differential transform method. Tuna and Kirca [22] studied free vibration and buckling of nonlocal Euler-Bernoulli beams utilizing the Laplace transform method. Hamza-Cherif et al. [23] employed a differential transform method to study the free vibration of a single-walled carbon nanotube resting on an elastic foundation under thermal effect. Aria and Friswell [24] used the finite element method to examine the free vibration and the buckling behavior of functionally graded Timoshenko nanobeams. Nikam and Sayyad [25] presented closed-form solutions for bending, buckling, and free vibration of simply supported nanobeams. Arian et al. [26] studied the effect of the thickness-to-length ratio on the frequency ratio of Timoshenko nanobeams and nanoplates. Ufuk [27] used the Ritz method in free transverse vibration analysis of cantilever nanobeam with intermediate support. Wang et al. [28] presented an analytical buckling analysis of micro and nano roads/tubes based on nonlocal Timoshenko beam theory. Reddy [29] reformulated Euler-Bernoulli, Timoshenko, Reddy, and Levinson beam theories using the nonlocal theory for bending, buckling, and vibrations of beams. Pradhan and Phadikar [30] solved buckling, bending, and vibration problems of nonhomogeneous nanotubes using the differential quadrature method. Aydogdu [31] proposed a generalized nonlocal beam theory to study the bending, buckling, and free vibration of nanobeams. Thai [32] presented analytical solutions for bending, buckling, and free vibration of nanobeams based on a nonlocal shear deformation beam theory. Eltaher et al. [33] used Galerkin finite element method to study static deflection and buckling response of functionally graded nanobeams for different combinations of boundary conditions. Ebrahimi and Salari [34] developed a differential transform method solution for vibrational and buckling analysis of functionally graded nanobeams considering the physical neutral axis position. Buckling analysis of two-directional functionally graded Euler-Bernoulli nanobeam has been presented by Nejad et al. [35] using the generalized differential quadrature method. Safarabadi et al. [36] studied the effect of surface energy on the free vibration of rotating nanobeam using the differential quadrature method. Mohammadi et al. [37] used the differential quadrature method to present the hygro-mechanical vibration of a rotating viscoelastic nanobeam resting on a visco-Pasternak foundation subjected to nonlinear temperature variation. An asymptotic solution for critical buckling load of Euler-Bernoulli nanobeam using Eringen's two-phase nonlocal theory has been presented by Zhu et al. [38]. Khaniki and Hosseini-Hashemi [39] presented a buckling analysis of tapered nanobeam using nonlocal strain gradient theory and the generalized differential quadrature method. Finite element analysis of bending, buckling, and free vibration problems of Euler-Bernoulli nanobeam has been presented by Tuna and Kirca [40] using Eringen's nonlocal integral model. Buckling analysis of nonuniform nonlocal strain gradient beams has been presented by Bakhshi et al. [41] using the generalized differential quadrature method. Stability analysis of simply supported nonlocal Euler-Bernoulli beam with varying cross-sections and resting on the Pasternak foundation has been presented by Soltani and Mohammadi [42]. Xu and Zheng [43] solved the buckling problem of the nonlocal strain gradient Timoshenko beam in closed form. The differential quadrature method and the

differential transform method have been used by Jena and Chakraverty [44] for the buckling analysis of nanobeams. Ragb et al. [45] obtained natural frequencies of a piezoelectric nanobeam resting on a nonlinear Pasternak foundation using different versions of the differential quadrature method. Nazmul and Devnath [46] derived closed-form solutions for bending and buckling of functionally graded nanobeam using the Laplace transform. Karmakar and Chakravarty [47] studied the thermal vibration of an Euler nanobeam resting on the Winkler-Pasternak foundation using the differential quadrature method and the Adomian decomposition method. Zewei et al. [48] used the differential quadrature method in free vibration, buckling, and dynamic stability analyses of Timoshenko micro/nanobeams resting on the Pasternak foundation under axial load. Civalek et al. [49] studied the stability of restrained FGM nonlocal beams using the Fourier series. Jalaei et al. [50] presented an analytical transient response of porous viscoelastic functionally graded nanobeam subjected to dynamic load and magnetic field. Beni [51] investigated free vibration and static torsion of an electromechanical flexoelectric micro/nanotube. Beni and Beni [52] studied the dynamic stability of an isotropic viscoelastic/piezoelectric Euler-Bernoulli nanobeam using the Galerkin method. Numanoğlu et al. [53] presented a thermo-mechanical vibration analysis of Timoshenko nanobeam using the nonlocal finite element method. Karmakar and Chakraverty [54] used the Adomian decomposition method and the homotopy perturbation method to study the thermal vibration of nonhomogeneous Euler nanobeam resting on the Winkler foundation.

This paper aims at providing a numerical solution for free transverse vibration and buckling of a nanobeam under axial load and resting on the Pasternak foundation. Eringen's nonlocal elasticity theory along with the Euler-Bernoulli beam theory is used to develop the mathematical model. The PDQM and the HDQM are used to obtain the first three frequencies and the lowest critical buckling loads for clamped-clamped (C-C), clamped-simply supported (C-S), and simply supported-simply supported (S-S) beams.

The impacts of nonlocal parameters, axial force, and elastic foundation moduli on frequencies are studied. The effects of nonlocal parameters, boundary conditions, and elastic foundation moduli on critical buckling load are also studied.

2. Formulation of the Problem

Consider an isotropic uniform nanobeam of length L, cross-section area A , density ρ, and transverse deflection $w(x,t)$ as shown in Fig. 1. Here, t denotes the time. The beam is resting on the Pasternak foundation and is also subjected to uniform compressive load p.

The fundamental assumptions of the Euler-Bernoulli beam theory (Abbas et al. [55]) are:

(i) The cross-section of the beam remains plane to the deformed axis of the beam.

(ii) Deformed angles of rotation of the neutral axis are small.

This theory does not account for the effect of transverse shear strain and overpredicts natural frequencies.

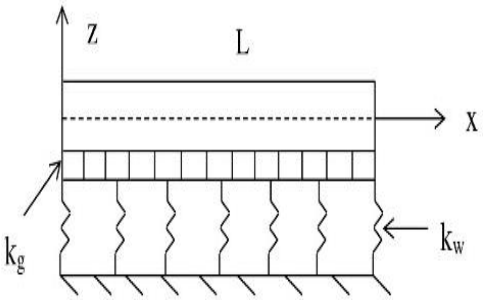

Fig. 1. Geometry of a Euler-Bernoulli nanobeam resting on Pasternak foundation

The strain energy of the beam is expressed as (Wang et al. [56]):

$$U = \frac{1}{2}\int_0^L \int_A \sigma_{xx}\varepsilon_{xx} dA dx \tag{1}$$

where σ_{xx} is normal stress.

Normal strain ε_{xx} in terms of deflection is represented as

$$\varepsilon_{xx} = -z\frac{d^2w}{dx^2}. \tag{2}$$

Using (2), strain energy given by (1) becomes

$$U = -\frac{1}{2}\int_0^L M\frac{d^2w}{dx^2}dx \tag{3}$$

where M is the bending moment and is defined as

$$M = \int_A z\sigma_{xx} dA. \tag{4}$$

The kinetic energy of the beam is expressed as (Wang et al. [56])

$$T = \frac{1}{2}\int_0^L \rho A\left(\frac{\partial w}{\partial t}\right)^2 dx. \quad (5)$$

The potential energy due to the Pasternak foundation is represented as

$$W_f = \frac{1}{2}\int_0^L \left(k_w w^2 + k_g\left(\frac{dw}{dx}\right)^2\right) dx \quad (6)$$

where k_w and k_g are the Winkler and the Pasternak (shear) foundation stiffnesses, respectively.

Work done by the compressive load p is expressed as

$$W_p = -\frac{1}{2}\int_0^L p\left(\frac{dw}{dx}\right)^2 dx. \quad (7)$$

Using Hamilton's principle

$$\int_0^t \delta(T - U - W_f - W_p)\, dt = 0 \quad (8)$$

The equation of motion of the beam is obtained as follows:

$$\frac{d^2M}{dx^2} + \left(k_g - p\right)\frac{d^2w}{dx^2} + (\rho A\omega^2 - k_w)w = 0. \quad (9)$$

Based on Eringen's nonlocal elasticity theory, the nonlocal stress tensor σ at a point x is given as (Murmu and Adhikari [57])

$$\sigma(x) = \int\int\int K(\lceil x - x'\rceil, \alpha)\ \tau\, dV(x') \quad (10)$$

where τ and $K(\lceil x - x'\rceil, \alpha)$ are classical stress and nonlocal modulus, respectively.

The differential form of the above integral constitutive relation (Murmu and Adhikari [57]) is

$$(1 - (e_0 a)^2\nabla^2)\,\sigma = \tau \quad (11)$$

where e_0 is a material constant, ∇^2 is the Laplace operator and a is the internal characteristic length.

For Euler-Bernoulli nanobeam, the relationship between local and nonlocal stresses (Eringen [5]) given by Eq. (11) can be rewritten as follows:

$$\sigma_{xx} - (e_0 a)^2\frac{d^2\sigma_{xx}}{dx^2} = E\varepsilon_{xx}. \quad (12)$$

Multiplying the equation (12) by $z\, dA$ and integrating over the area A, we obtain

$$M - (e_0 a)^2\frac{d^2M}{dx^2} = -EI\frac{d^2w}{dx^2} \quad (13)$$

where E is Young's modulus and

$$I = \int_A z^2 dA \quad (14)$$

is the second moment of the area.

By using Eqs. (9) and (13), the equation of motion is obtained as follows:

$$\left(1 + {L_i}^2\left(K_g - P\right)\right)\frac{d^4W}{dX^4} + \left(P + {L_i}^2(\Omega^2 - K_w) - K_g\right)\frac{d^2W}{dX^2} + (K_w - \Omega^2)W = 0 \quad (15)$$

where $X = \frac{x}{L}$, $W = \frac{w}{L}$, $l_i = e_0 a$, $P = \frac{pL^2}{EI}$, $K_w = \frac{k_w L^4}{EI}$, $K_g = \frac{k_g L^2}{EI}$, $L_i = \left(\frac{e_0 a}{L}\right)$ is the nonlocal parameter and $\Omega = \omega L^2\sqrt{\frac{\rho A}{EI}}$ is the frequency parameter.

The buckling problem is obtained by putting $\Omega = 0$ in Eq. (15) and is given as follows:

$$\left(1 + {L_i}^2\left(K_g - P_{cr}\right)\right)\frac{d^4W}{dX^4} + \left(P_{cr} - {L_i}^2K_w - K_g\right)\frac{d^2W}{dX^2} + K_w W = 0 \quad (16)$$

where P_{cr} is the critical buckling load.

2.1. Boundary Conditions

Boundary conditions at the ends $X = 0$ and $X = 1$ are given as

For C-C beam

$$W(0) = 0, \frac{dW(0)}{dX} = 0. \qquad W(1) = 0, \frac{dW(1)}{dX} = 0. \quad (17a\text{-}17d)$$

For C-S beam

$$W(0) = 0, \frac{dW(0)}{dX} = 0 \qquad W(1) = 0, \qquad \left(1 - {L_i}^2\left(P - K_g\right)\right)\frac{d^2W(1)}{dX^2} + {L_i}^2(\Omega^2 - K_w)W(1) = 0. \quad (18a - 18d)$$

For S-S beam

$$W(0) = 0, \qquad \left(1 - {L_i}^2\left(P - K_g\right)\right)\frac{d^2W(0)}{dX^2} + {L_i}^2(\Omega^2 - K_w)W(0) = 0. \quad (19a\text{-}19d)$$

$W(1) = 0,$

$$\left(1 - {L_i}^2\left(P - K_g\right)\right)\frac{d^2W(1)}{dX^2}$$

$$+{L_i}^2(\Omega^2 - K_w)W(1) = 0.$$

Using the PDQM and the HDQM, free vibration and buckling problems are reduced to eigenvalue problems which are solved for frequencies and critical buckling loads, respectively.

2.2. PDQM (Bert and Malik [58])

The displacement W and its derivatives are approximated by a weighted linear sum of functional values at grid points $0 = X_1 < X_2 < \cdots < X_N = 1$ as follows:

$$\frac{d^mW(X_i)}{dX^m} = \sum_{j=1}^{N} {C_{ij}}^{(m)} W(X_j) \tag{20}$$

$${C_{ij}}^{(1)} = \frac{M(X_i)}{(X_i - X_j)M(X_j)} \tag{21}$$

$$M(X_i) = \prod_{\substack{j=1 \\ j\neq i}}^{N}\left(X_i - X_j\right) \tag{22}$$

$i = 1,2,3, \ldots, N \quad \text{and} \quad i \neq j.$

$${C_{ij}}^{(m)} = m\left({C_{ii}}^{(m-1)}{C_{ij}}^{(1)} - \frac{{C_{ij}}^{(m-1)}}{\left(X_i - X_j\right)}\right) \tag{23}$$

$i \neq j \quad \text{and} \quad m = 2,3, \ldots, N-1.$

$${C_{ii}}^{(m)} = -\sum_{\substack{j=1 \\ j\neq i}}^{N} {C_{ij}}^{(m)} \tag{24}$$

$i = 1,2,3, \ldots, N \quad \text{and}$

$m = 1,2, \ldots, N-1.$

2.3. HDQM (Civalek [59])

In this method, the weighting coefficients of the first, second, third, and fourth order derivatives are obtained as follows:

$${C_{ij}}^{(1)} = \frac{\left(\frac{\pi}{2}\right)M(X_i)}{M\left(X_j\right)sin\left[\frac{\left(X_i - X_j\right)\pi}{2}\right]} \tag{25}$$

$$M(X_i) = \prod_{j=1, j\neq i}^{N} sin\left[\frac{\left(X_i - X_j\right)\pi}{2}\right] \tag{26}$$

$${C_{ij}}^{(2)} = {C_{ij}}^{(1)}\left[\begin{matrix} 2{C_{ii}}^{(1)} - \\ \pi\, cot\left\{\frac{\left(X_i - X_j\right)\pi}{2}\right\}\end{matrix}\right] \tag{27}$$

$i, j = 1,2,3, \ldots, N \quad \text{and} \quad i \neq j.$

$${C_{ii}}^{(p)} = -\sum_{j=1, j\neq i}^{N} {C_{ij}}^{(p)}, p = 1 \; or \; 2 \tag{28}$$

$${C_{ij}}^{(3)} = \sum_{k=1}^{N} {C_{ik}}^{(1)}\,{C_{kj}}^{(2)} \tag{29}$$

$${C_{ij}}^{(4)} = \sum_{k=1}^{N} {C_{ik}}^{(2)}\,{C_{kj}}^{(2)} \tag{30}$$

$i, j = 1,2,3, \ldots, N.$

The Gauss-Chebyshev-Lobatto grid points (Chang [60]) in the range [0, 1] are given below as:

$$X_i = \frac{1}{2}\left[1 - cos\left(\frac{i-1}{N-1}\pi\right)\right] \tag{31}$$

$i = 1,2,3, \ldots, N.$

We obtain a set of $(N-4)$ equations in N unknowns $X_1, X_2, \ldots, X_N$ by discretizing the equation of motion (15) at grid points X_i $(i = 3,4, \ldots, N-2)$ as follows:

$$\begin{aligned}&\left(1 + {L_i}^2\left(K_g - P\right)\right)\sum_{j=1}^{N} {C_{ij}}^{(4)} W\left(X_j\right) \\ &+\left(P + {L_i}^2(\Omega^2 - K_w) - K_g\right) \\ &\times \sum_{j=1}^{N} {C_{ij}}^{(2)} W\left(X_j\right) \\ &+(K_w - \Omega^2)W(X_i) = 0,\end{aligned} \tag{32}$$

Similarly, the buckling problem (16) can be discretized as follows:

$$\begin{aligned}&\left(1 + {L_i}^2\left(K_g - P_{cr}\right)\right)\sum_{j=1}^{N} {C_{ij}}^{(4)} W\left(X_j\right) \\ &+\left(P_{cr} - {L_i}^2 K_w - K_g\right)\sum_{j=1}^{N} {C_{ij}}^{(2)} W\left(X_j\right) \\ &+K_w W(X_i) = 0.\end{aligned} \tag{33}$$

By discretizing boundary conditions (17a-17d) for the C-C beam, we obtain a set of four equations in N unknowns $X_1, X_2, \ldots, X_N$

$$W(0)=0,\ \sum_{j=1}^{N} {C_{1j}}^{(1)} W(X_j)=0,$$
$$W(1)=0,\ \sum_{j=1}^{N} {C_{Nj}}^{(1)} W(X_j)=0. \quad \text{(34a-34d)}$$

Equations (32) and (34a-34d) form a set of N algebraic linear equations in N unknowns. This set represents a generalized eigenvalue problem that is solved to obtain frequencies for the C-C beam.

The boundary conditions for C-S and S-S beams are discretized as

$$W(0)=0,$$
$$\sum_{j=1}^{N} {C_{1j}}^{(1)} W(X_j)=0,$$
$$W(1)=0, \quad \text{(35a-35d)}$$
$$\left(1-{L_i}^2(P-K_g)\right)\sum_{j=1}^{N} {C_{Nj}}^{(2)} W(X_j)$$
$$+{L_i}^2(\Omega^2-K_w)W(1)=0.$$

and

$$W(0)=0,$$
$$\left(1-{L_i}^2(P-K_g)\right)\sum_{j=1}^{N} {C_{1j}}^{(2)} W(X_j)$$
$$+{L_i}^2(\Omega^2-K_w)W(0)=0, \quad \text{(36a-36d)}$$
$$W(1)=0,$$
$$\left(1-{L_i}^2(P-K_g)\right)\sum_{j=1}^{N} {C_{Nj}}^{(2)} W(X_j)$$
$$+{L_i}^2(\Omega^2-K_w)W(1)=0.$$

Similarly, critical buckling loads for C-C, C-S and S-S beams can be obtained by using equation (33) and discretizing boundary conditions represented by equations (17a-17d), (18a-18d), and (19a-19d), respectively.

3. Results and Discussion

The first three frequencies and the lowest critical buckling loads are calculated by solving the corresponding eigenvalue problem and the buckling problem, respectively. The Convergence of results for both versions of DQM with an increasing number of grid points is shown in Tables 1 and 2 for $L_i=0.1$, $P=3, K_w=100, K_g=10$. The value of N has been fixed as 17 as we get results correct to four decimal places. Results are shown in the Tables (3-6).

Tables (3-5) present the first three frequencies while Table 6 shows critical buckling loads for C-C, C-S, and S-S nanobeams for different combinations of parameters. A comparison of frequencies in special cases is presented in Table (7) while a comparison of critical buckling loads in special cases is shown in Table (8). It is evident from the comparison tables that the results are in good agreement with those available in the literature.

Table 1. Convergence of frequency parameter $\boldsymbol{\Omega}$ of Euler-Bernoulli nanobeam using PDQM

$L_i=0.1, P=3, K_w=100, K_g=10$						
	N					
	10	13	14	15	16	17
Mode				C-C		
I	5.0562	5.0562	5.0562	5.0562	5.0562	5.0562
II	7.4587	7.4640	7.4640	7.4640	7.4640	7.4640
III	9.6622	9.5491	9.5481	9.5475	9.5475	9.5475
				C-S		
I	4.4727	4.4728	4.4728	4.4728	4.4728	4.4728
II	6.8302	6.8326	6.8325	6.8325	6.8325	6.8325
III	9.2086	8.9567	8.9573	8.9560	8.9560	8.9560
				S-S		
I	4.0068	4.0068	4.0068	4.0068	4.0068	4.0068
II	6.2130	6.2169	6.2169	6.2169	6.2169	6.2169
III	8.5510	8.3685	8.3675	8.3667	8.3667	8.3667

Table 2. Convergence of frequency parameter $\boldsymbol{\Omega}$ of Euler-Bernoulli nanobeam using HDQM

$L_i = 0.1, P = 3, K_w = 100, K_g = 10$						
				N		
	10	13	14	15	16	17
Mode				C-C		
I	5.0650	5.0564	5.0566	5.0563	5.0562	5.0562
II	7.4664	7.4651	7.4640	7.4641	7.4640	7.4640
III	9.5614	9.5477	9.548	9.5475	9.5475	9.5475
				C-S		
I	4.4859	4.4702	4.4737	4.4722	4.4730	4.4728
II	6.8247	6.8355	6.8316	6.8332	6.8323	6.8325
III	8.9794	8.9547	8.9572	8.9556	8.9563	8.9560
				S-S		
I	3.9863	4.0068	4.0056	4.0068	4.0065	4.0068
II	6.2266	6.2169	6.2173	6.2169	6.2169	6.2169
III	8.3869	8.3667	8.3675	8.3667	8.3669	8.3667

Table 3. First three values of frequency parameter $\boldsymbol{\Omega}$ of C-C Euler-Bernoulli nanobeam

							L_i				
			0		0.1		0.2		0.3		0.4	
							P					
K_w	K_g	Mode	-3	3	-3	3	-3	3	-3	3	-3	3
1	0	I	4.8170	4.6427	4.7119	4.4725	4.4740	4.0547	4.2233	3.5302	4.0158	2.9427
		II	7.9240	7.7814	7.2571	7.0188	6.2603	5.7842	5.5576	4.7433	5.1047	3.8372
		III	11.0512	10.9396	9.3728	9.1401	7.6302	7.1119	6.6414	5.7228	6.0581	4.6072
	10	I	5.0692	4.9229	5.0431	4.8528	4.9852	4.6988	4.9273	4.5449	4.8830	4.4251
		II	8.1452	8.0148	7.6084	7.4037	6.8721	6.5259	6.4215	5.9490	6.1701	5.6052
		III	11.2299	11.1237	9.7262	9.5189	8.3129	7.9246	7.6364	7.0905	7.3007	6.6405
	30	I	5.4780	5.3657	5.5558	5.4172	5.6941	5.5092	5.8005	5.5797	5.8676	5.6238
		II	8.5381	8.4262	8.1924	8.0304	7.7561	7.5225	7.5171	7.2384	7.3947	7.0906
		III	11.5632	11.4663	10.3357	10.1642	9.3206	9.0525	8.9129	8.5873	8.7377	8.3804
	50	I	5.8067	5.7145	5.9546	5.8436	6.2073	6.0667	6.3970	6.2356	6.5156	6.3415
		II	8.8809	8.7824	8.6724	8.5368	8.4120	8.2313	8.2736	8.0684	8.2043	7.9865
		III	11.8693	11.7800	10.8533	10.7058	10.0788	9.8693	9.7993	9.5586	9.6901	9.4338
10	0	I	4.8370	4.6650	4.7333	4.4975	4.4989	4.0881	4.2529	3.5802	4.0501	3.0273
		II	7.9285	7.7862	7.2630	7.0253	6.2695	5.7958	5.5707	4.7642	5.1215	3.8764
		III	11.0528	10.9413	9.3756	9.1430	7.6353	7.1181	6.6491	5.7348	6.0682	4.6301
	10	I	5.0864	4.9416	5.0606	4.8724	5.0033	4.7204	4.9461	4.5687	4.9022	4.4509
		II	8.1494	8.0192	7.6135	7.4093	6.8790	6.5340	6.4299	5.9597	6.1797	5.6180
		III	11.2315	11.1253	9.7286	9.5215	8.3168	7.9292	7.6415	7.0968	7.3065	6.6482
	30	I	5.4917	5.3802	5.5689	5.4313	5.7062	5.5226	5.8120	5.5926	5.8787	5.6365
		II	8.5417	8.4299	8.1965	8.0347	7.7609	7.5278	7.5224	7.2443	7.4002	7.0970
		III	11.5646	11.4678	10.3378	10.1663	9.3234	9.0556	8.9161	8.5908	8.7410	8.3842
	50	I	5.8182	5.7265	5.9653	5.8548	6.2167	6.0768	6.4056	6.2448	6.5237	6.3503
		II	8.8841	8.7858	8.6758	8.5404	8.4158	8.2354	8.2776	8.0727	8.2084	7.9909
		III	11.8707	11.7814	10.8551	10.7077	10.0810	9.8716	9.8017	9.5612	9.6926	9.4365
1000	0	I	6.2618	6.1852	6.2150	6.1160	6.1165	5.9689	6.0243	5.8288	5.9568	5.7247
		II	8.3843	8.2646	7.8372	7.6506	7.0957	6.7842	6.6478	6.2287	6.4003	5.9049
		III	11.2317	11.1255	9.6624	9.4509	8.1392	7.7229	7.3664	6.7465	6.9595	6.1704
	10	I	6.3824	6.3110	6.3694	6.2782	6.3409	6.2093	6.3131	6.1448	6.2922	6.0976
		II	8.5725	8.4612	8.1213	7.9545	7.5384	7.2825	7.2080	6.8884	7.0342	6.6758
		III	11.4022	11.3009	9.9869	9.7961	8.7172	8.3848	8.1443	7.7062	7.8719	7.3657
	30	I	6.6018	6.5387	6.6467	6.5673	6.7290	6.6197	6.7943	6.6607	6.8365	6.6868
		II	8.9138	8.8158	8.6131	8.4744	8.2434	8.0509	8.0465	7.8224	7.9472	7.7063
		III	11.7214	11.6285	10.5549	10.3941	9.6148	9.3719	9.2465	8.9571	9.0901	8.7759
	50	I	6.7982	6.7414	6.8920	6.8213	7.0595	6.9652	7.1907	7.0787	7.2751	7.1518
		II	9.2178	9.1300	9.0323	8.9127	8.8034	8.6466	8.6831	8.5068	8.6233	8.4372
		III	12.0160	11.9299	11.0436	10.9038	10.3143	10.1194	10.0545	9.8326	9.9536	9.7182

Table 4. First three values of frequency parameter $\boldsymbol{\Omega}$ of C-S Euler-Bernoulli nanobeam

			L_i									
			0		0.1		0.2		0.3		0.4	
			P									
K_w	K_g	Mode	-3	3	-3	3	-3	3	-3	3	-3	3
1	0	I	4.0655	3.7797	3.9825	3.6454	3.7920	3.3102	3.5875	2.8782	3.4149	2.3753
		II	7.1586	6.9764	6.5937	6.3298	5.7313	5.2570	5.1121	4.3304	4.7087	3.5081
		III	10.2760	10.1435	8.7705	8.5286	7.1604	6.6543	6.2284	5.3495	5.6740	4.2981
	10	I	4.4351	4.2257	4.4020	4.1661	4.3280	4.0326	4.2531	3.8955	4.1945	3.7858
		II	7.4343	7.2727	6.9738	6.7535	6.3289	5.9920	5.9283	5.4830	5.7039	5.1771
		III	10.4861	10.3616	9.1342	8.9213	7.8214	7.4461	7.1736	6.6556	6.8449	6.2233
	30	I	4.9708	4.8292	4.9924	4.8377	5.0270	4.8478	5.0497	4.8500	5.0621	4.8483
		II	7.9073	7.7745	7.5880	7.4194	7.1786	6.9553	6.9549	6.6943	6.8427	6.5603
		III	10.8717	10.7604	9.7535	9.5801	8.7899	8.5329	8.3815	8.0736	8.1961	7.8604
	50	I	5.3684	5.2589	5.4239	5.3054	5.5165	5.3833	5.5854	5.4409	5.6287	5.4767
		II	8.3066	8.1930	8.0812	7.9428	7.8028	7.6313	7.6607	7.4694	7.5943	7.3922
		III	11.2198	11.1188	10.2733	10.1256	9.5151	9.3149	9.2184	8.9913	9.0909	8.8502
10	0	I	4.0985	3.8207	4.0176	3.6910	3.8326	3.3706	3.6352	2.9682	3.4701	2.5278
		II	7.1648	6.9830	6.6016	6.3387	5.7432	5.2724	5.1288	4.3578	4.7301	3.5591
		III	10.2781	10.1457	8.7738	8.5322	7.1665	6.6619	6.2377	5.3641	5.6863	4.3261
	10	I	4.4606	4.2552	4.4281	4.1969	4.3555	4.0665	4.2820	3.9330	4.2247	3.8266
		II	7.4398	7.2786	6.9805	6.7608	6.3378	6.0025	5.9391	5.4966	5.7160	5.1932
		III	10.4880	10.3636	9.1371	8.9245	7.8261	7.4516	7.1797	6.6632	6.8519	6.2326
	30	I	4.9890	4.8490	5.0104	4.8574	5.0446	4.8674	5.0671	4.8696	5.0794	4.8679
		II	7.9118	7.7792	7.5932	7.4249	7.1847	6.9620	6.9615	6.7018	6.8497	6.5682
		III	10.8735	10.7622	9.7559	9.5826	8.7932	8.5365	8.3853	8.0779	8.2002	7.8650
	50	I	5.3829	5.2743	5.4380	5.3205	5.5298	5.3977	5.5983	5.4548	5.6413	5.4903
		II	8.3105	8.1971	8.0855	7.9472	7.8076	7.6363	7.6657	7.4748	7.5994	7.3977
		III	11.2214	11.1205	10.2754	10.1278	9.5177	9.3177	9.2213	8.9943	9.0939	8.8534
1000	0	I	5.9722	5.8895	5.9467	5.8555	5.8927	5.7838	5.8418	5.7162	5.8043	5.6663
		II	7.7595	7.6179	7.3316	7.1437	6.7516	6.4796	6.4040	6.0623	6.2136	5.8240
		III	10.4988	10.3748	9.1193	8.9055	7.7608	7.3758	7.0738	6.5297	6.7169	6.0506
	10	I	6.1014	6.0251	6.0888	6.0049	6.0614	5.9620	6.0347	5.9212	6.0145	5.8911
		II	7.9792	7.8496	7.6159	7.4493	7.1431	6.9162	6.8751	6.6047	6.7350	6.4375
		III	10.6963	10.5792	9.4456	9.2540	8.2980	7.9888	7.7712	7.3768	7.5178	7.0703
	30	I	6.3339	6.2673	6.3444	6.2712	6.3614	6.2759	6.3727	6.2769	6.3789	6.2761
		II	8.3702	8.2588	8.1045	7.9672	7.7752	7.6017	7.6014	7.4053	7.5161	7.3073
		III	11.0611	10.9555	10.0122	9.8523	9.1366	8.9092	8.7768	8.5113	8.6163	8.3307
	50	I	6.5402	6.4806	6.5711	6.5057	6.6239	6.5484	6.6641	6.5807	6.6897	6.6010
		II	8.7117	8.6136	8.5178	8.4001	8.2825	8.1401	8.1644	8.0077	8.1096	7.9452
		III	11.3926	11.2962	10.4963	10.3581	9.7926	9.6096	9.5219	9.3167	9.4065	9.1903

Table 5. First three values of frequency parameter $\boldsymbol{\Omega}$ of S-S Euler-Bernoulli nanobeam

			L_i									
			0		0.1		0.2		0.3		0.4	
			P									
K_w	K_g	Mode	-3	3	-3	3	-3	3	-3	3	-3	3
1	0	I	3.3637	2.8800	3.3047	2.7837	3.1658	2.5340	3.0110	2.1894	2.8756	1.7397
		II	6.4002	6.1613	5.9303	5.6234	5.1867	4.6973	4.6355	3.8724	4.2700	3.1268
		III	9.5037	9.3445	8.1657	7.9091	6.6878	6.1893	5.8167	4.9733	5.2951	3.9890
	10	I	3.8803	3.5975	3.8423	3.5496	3.7566	3.4393	3.6674	3.3212	3.5952	3.2226
		II	6.7474	6.5458	6.3556	6.1112	5.7831	5.4491	5.4099	4.9893	5.1930	4.7058
		III	9.7524	9.6055	8.5461	8.3242	7.3312	6.9668	6.7148	6.2233	6.3968	5.8125
	30	I	4.5380	4.3706	4.5145	4.3442	4.4624	4.2856	4.4102	4.2264	4.3693	4.1799
		II	7.3144	7.1582	7.0147	6.8364	6.6092	6.3938	6.3696	6.1270	6.2407	5.9813
		III	10.1995	10.0716	9.1829	9.0058	8.2645	8.0176	7.8563	7.5658	7.6645	7.3497
	50	I	4.9930	4.8695	4.9753	4.8505	4.9367	4.8087	4.8983	4.7672	4.8686	4.7349
		II	7.7737	7.6445	7.5275	7.3847	7.2069	7.0432	7.0251	6.8477	6.9300	6.7448
		III	10.5946	10.4807	9.7094	9.5605	8.9588	8.7675	8.6452	8.4312	8.5030	8.2775
10	0	I	3.4213	2.9699	3.3653	2.8827	3.2345	2.6622	3.0903	2.3780	2.9659	2.0643
		II	6.4088	6.1709	5.9411	5.6360	5.2028	4.7189	4.6580	3.9106	4.2987	3.1979
		III	9.5063	9.3472	8.1698	7.9137	6.6953	6.1988	5.8281	4.9915	5.3102	4.0240
	10	I	3.9183	3.6449	3.8814	3.5989	3.7983	3.4934	3.7122	3.3810	3.6427	3.2879
		II	6.7547	6.5538	6.3643	6.1210	5.7947	5.4629	5.4240	5.0073	5.2090	4.7272
		III	9.7549	9.6080	8.5497	8.3280	7.3369	6.9734	6.7222	6.2327	6.4054	5.8240
	30	I	4.5619	4.3973	4.5387	4.3713	4.4875	4.3139	4.4362	4.2559	4.3961	4.2104
		II	7.3202	7.1643	7.0212	6.8435	6.6170	6.4024	6.3783	6.1367	6.2499	5.9918
		III	10.2017	10.0738	9.1858	9.0088	8.2685	8.0220	7.8609	7.5710	7.6695	7.3554
	50	I	5.0110	4.8889	4.9935	4.8701	4.9553	4.8288	4.9173	4.7878	4.8880	4.7560
		II	7.7785	7.6495	7.5328	7.3903	7.2129	7.0496	7.0316	6.8547	6.9367	6.7521
		III	10.5965	10.4827	9.7119	9.5630	8.9619	8.7708	8.6487	8.4349	8.5067	8.2814
1000	0	I	5.7941	5.7164	5.7828	5.7047	5.7583	5.6791	5.7342	5.6541	5.7158	5.6349
		II	7.1930	7.0283	6.8764	6.6866	6.4425	6.2086	6.1822	5.9147	6.0406	5.7519
		III	9.7821	9.6366	8.5901	8.3717	7.4005	7.0472	6.8044	6.3352	6.5001	5.9486
	10	I	5.9169	5.8441	5.9064	5.8332	5.8834	5.8093	5.8609	5.7859	5.8436	5.7680
		II	7.4447	7.2968	7.1617	6.9947	6.7835	6.5853	6.5632	6.3429	6.4458	6.2123
		III	10.0112	9.8757	8.9209	8.7270	7.8963	7.6105	7.4205	7.0704	7.1906	6.8018
	30	I	6.1420	6.0771	6.1325	6.0673	6.1120	6.0461	6.0919	6.0254	6.0766	6.0095
		II	7.8829	7.7591	7.6474	7.5114	7.3428	7.1885	7.1715	7.0053	7.0822	6.9093
		III	10.4272	10.3076	9.4897	9.3298	8.6753	8.4636	8.3273	8.0863	8.1675	7.9111
	50	I	6.3447	6.2859	6.3361	6.2771	6.3176	6.2580	6.2994	6.2393	6.2855	6.2250
		II	8.2582	8.1510	8.0550	7.9392	7.7974	7.6694	7.6555	7.5199	7.5824	7.4427
		III	10.7986	10.6912	9.9715	9.8343	9.2876	9.1166	9.0082	8.8202	8.8830	8.6865

Table 6. Critical buckling load parameter P_{cr} of Euler-Bernoulli nanobeam

		L_i				
		0	0.1	0.2	0.3	0.4
K_w	K_g			C-C		
1	0	39.5544	28.3659	15.3518	10.3878	5.4280
	30	69.5544	58.3659	45.3518	40.3878	35.4280
	50	89.5544	78.3659	65.3518	60.3878	55.4280
10	0	40.2376	28.9201	15.7558	10.4530	6.0810
	30	70.2376	58.9201	45.7558	40.4530	36.0810
	50	90.2376	78.9201	65.7558	60.4530	56.0810
1000	0	101.1910	61.2950	28.6333	13.6863	7.8113
	30	131.1910	91.2950	58.6333	43.6863	37.8113
	50	151.1910	111.2950	78.6333	63.6863	57.8113
				C-S		
1	0	20.2733	16.8759	11.2375	7.2283	4.8300
	30	50.2733	46.8759	41.2375	37.2283	34.8300
	50	70.2733	66.8759	61.2375	57.2283	54.8300
10	0	21.0149	17.5676	11.8463	7.7780	6.1985
	30	51.0149	47.5676	41.8463	37.7780	36.1985
	50	71.0149	67.5676	61.8463	57.7780	56.1985
1000	0	74.4955	55.8308	25.0525	12.7116	7.3664
	30	104.4950	85.8308	55.0525	42.7116	37.3664
	50	124.4950	105.8310	75.0525	62.7116	57.3664
				S-S		
1	0	9.9709	9.0843	7.1774	5.3282	3.9280
	30	39.9709	39.0843	37.1774	35.3282	33.9280
	50	59.9709	59.0843	57.1774	55.3282	53.9280
10	0	10.8828	9.9963	8.0893	6.2400	4.8399
	30	40.8828	39.9962	38.0893	36.2400	34.8399
	50	60.8828	59.9962	58.0893	56.2400	54.8399
1000	0	64.8087	53.6346	25.8330	12.3344	6.9380
	30	94.8087	83.6346	55.8330	42.3344	36.9380
	50	114.8087	103.6346	75.8330	62.3344	56.9380

Table 7. Comparison of frequency parameter Ω of Euler-Bernoulli nanobeam

Boundary condition	Reference	K_w	K_g	L_i	Mode I	Mode II	Mode III
C-C	Demir [61]	0	0	0	4.73004	7.8532	11.0856
	Ebrahimi and Salari [34]				4.7299	7.8525	10.9934
	Present				**4.7300**	**7.8532**	**10.9956**
	Demir [61]	0	0	0.05	4.69433	7.64178	10.4625
	Present				**4.6943**	**7.6418**	**10.4042**
	Demir [61]	0	0	0.2	4.27661	6.03520	7.28636
	Present				**4.2766**	**6.0352**	**7.3840**
	Demir [61]	10000	0	0.2	10.08260	10.31634	10.64047
	Present				**10.0826**	**10.3163**	**10.6723**
	Rahbar-Ranji and Shahbaztabar [62]	2.5	$2.5*\pi^2$	0	5.3200	8.3815	11.4280
	Present				**5.3224**	**8.3821**	**11.4282**
	Rahbar-Ranji and Shahbaztabar [62]	10000	$2.5*\pi^2$	0	10.1943	11.0546	12.8252
	Present				**10.1943**	**11.0546**	**12.8251**
C-S	Wang, Zhang, and He [10]	0	0	0	3.9266	7.0686	10.2102
	Ebrahimi and Salari [34]				3.9265	7.0679	10.2081
	Present				**3.9266**	**7.0686**	**10.2102**
	Wang, Zhang, and He [10]	0	0	0.3	3.2828	4.7668	5.8371
	Present				**3.28284**	**4.7668**	**5.8371**
	Wang, Zhang, and He [10]	0	0	0.5	2.7899	3.8325	4.6105
	Present				**2.7899**	**3.8325**	**4.6105**
S-S	Demir [61]	0	0	0	3.14159	6.28319	9.42394
	Present				**3.1416**	**6.2832**	**9.4248**
	Demir [61]	0	0	0.05	3.12251	6.13706	8.96310
	Present				**3.1225**	**6.1371**	**8.9639**
	Demir [61]	0	0	0.2	2.89083	4.95805	6.45140
	Present				**2.8908**	**4.9581**	**6.4520**
	Demir [61]	10000	0	0.2	10.01741	10.14776	10.40748
	Present				**10.0174**	**10.1478**	**10.4076**
	Rahbar-Ranji and Shahbaztabar [62]	10000	$2.5*\pi^2$	0	10.0842	10.5806	11.9042
	Present				**10.0842**	**10.5806**	**11.9042**

Table 8. Comparison of the lowest non-dimensional critical buckling load parameter $\boldsymbol{P_{cr}}$ for Euler-Bernoulli nanobeam without foundation

Boundary condition	Reference	L_i	P_{cr}
C-C	Ghannadpour, Mohammadi, and Fazilati [63]	0	39.4784
	Pradhan and Phadikar [30]		39.4784
	Nejad, Hadi and Rastgoo [35]		39.4784
	Zhu, Wang and Dai [38]		39.47842
	Present		**39.4784**
	Ghannadpour, Mohammadi, and Fazilati [63]	0.2	15.3068
	Nejad, Hadi and Rastgoo [35]		15.3068
	Present		**15.3069**
C-S	Ghannadpour, Mohammadi, and Fazilati [63]	0	20.1907
	Pradhan and Phadikar [30]		20.1907
	Nejad, Hadi and Rastgoo [35]		20.1907
	Zhu, Wang and Dai [38]		20.19073
	Present		**20.1907**
	Ghannadpour, Mohammadi, and Fazilati [63]	0.2	11.1697
	Nejad, Hadi and Rastgoo [35]		11.1697
	Present		**11.1697**
S-S	Sari, Al-Kouz and Atieh [64]	0	9.8696
	Reddy [29]		9.8696
	Ebrahimi and Salari [34]		9.8696044
	Eltaher, Emam and Mahmoud [33]		9.86973
	Wang and Cai [3]		9.8696
	Nejad, Hadi and Rastgoo [35]		9.8696
	Zhu, Wang and Dai [38]		9.86960
	Present		**9.8696**
	Sari, Al-Kouz and Atieh [64]	0.1	8.9830
	Reddy [29]		8.9830
	Eltaher, Emam and Mahmoud [33]		8.98312
	Present		**8.9830**
	Sari, Al-Kouz and Atieh [64]	$\sqrt{2}/10$	8.2426
	Reddy [29]		8.2426
	Eltaher, Emam and Mahmoud [33]		8.24267
	Present		**8.2426**
	Sari, Al-Kouz and Atieh [64]	0.2	7.0762
	Reddy [29]		7.0761
	Eltaher, Emam and Mahmoud [33]		7.07614
	Nejad, Hadi and Rastgoo [35]		7.076
	Present		**7.0761**
	Sari, Al-Kouz and Atieh [64]	$\sqrt{5}/10$	6.6085
	Reddy [29]		6.6085
	Present		**6.6084**

The first three frequencies and critical buckling loads are also presented through graphs via Figs. (2-9). The effect of nonlocal parameter L_i along with the shear foundation parameter on frequency Ω is shown in Figs. (2-3) for $P = 3$, $K_w = 10$ for C-C and C-S beams, respectively.

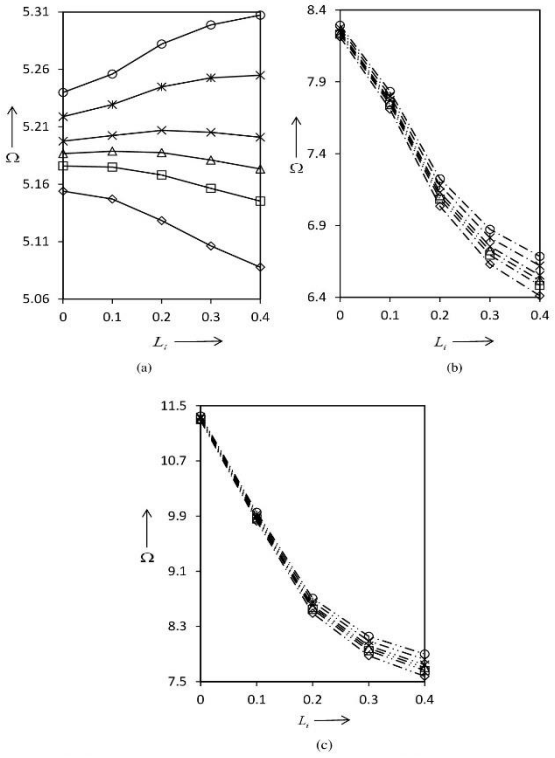

Fig. 2. (a)First mode (b) second mode (c) third mode of C-C nanobeam for $P = 3, K_w = 10$ *and* $K_g = 19(\diamond); K_g = 20(\square)$; $K_g = 20.5(\triangle)$; $K_g = 21(\times)$; $K_g = 22(*)$; $K_g = 23(\circ)$

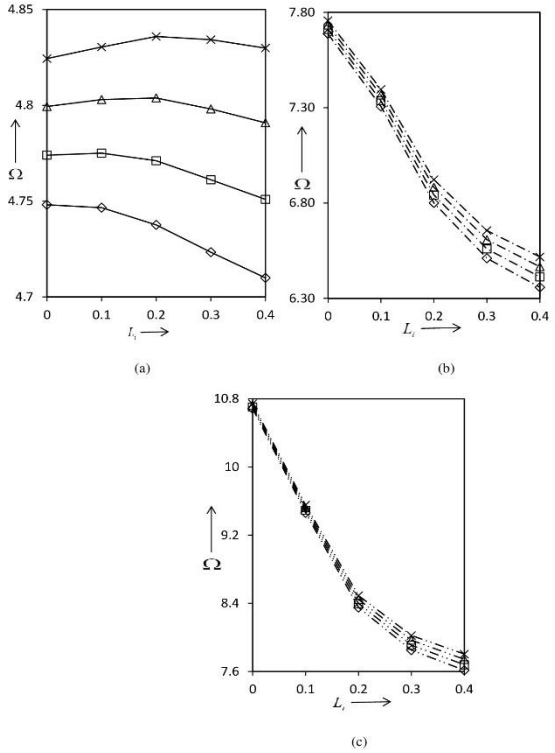

Fig. 3. (a)First mode (b) second mode (c) third mode of C-S nanobeam for $P = 3$, $K_w = 10$ *and* $K_g = 26$ ($\diamond$); $K_g = 27$ ($\square$); $K_g = 28$ ($\triangle$); $K_g = 29$ ($\times$)

Figure 4 shows the variation of frequency with respect to nonlocal parameters for different combinations of Winkler and shear foundation parameters.

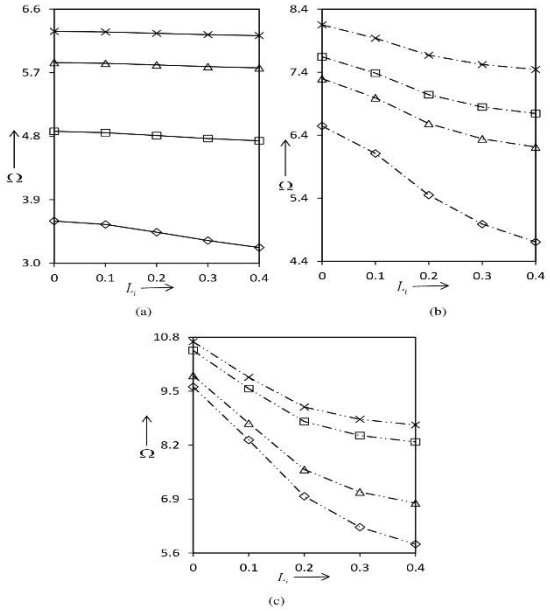

Fig. 4. (a)First mode (b) second mode (c) third mode of S-S nanobeam for $P = 3, and\ K_w = 1$, $K_g = 10$ ($\diamond$); $K_w = 1$, $K_g = 50$ ($\square$); $K_w = 1000$, $K_g = 10$ (Δ); $K_w = 1000$, $K_g = 50$ ($\times$)

The effect of the nonlocal parameter along with the Winkler foundation parameter on frequency is shown in Figs. (5-6) for C-C and C-S beams for fixed values of load parameter and shear foundation parameter.

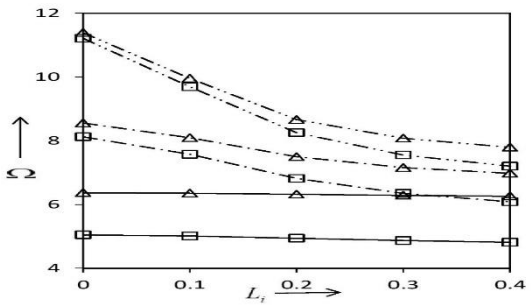

Fig. 5. First three modes of C-C nanobeam for $P = 3$, $K_g = 15$ *and* $K_w = 1(\square)$; $K_w = 1000(\triangle)$; First mode —; second mode - - - -; third mode - · - · -

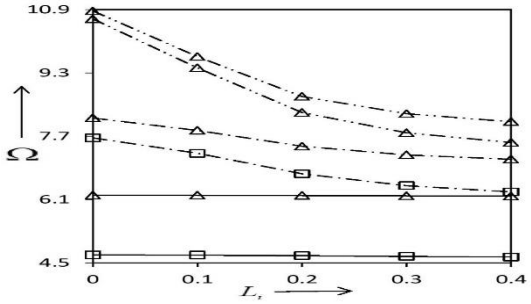

Fig. 6. First three modes of C-S nanobeam for $P = 3, K_g = 25$ *and* $K_w = 1(\square)$; $K_w = 1000(\triangle)$; First mode —; second mode - - - -; third mode - · - · -

Figure 7 shows the effect of the nonlocal parameter along with the shear foundation parameter on critical buckling loads for two different values of the Winkler foundation parameter for C-C, C-S, and S-S beams.

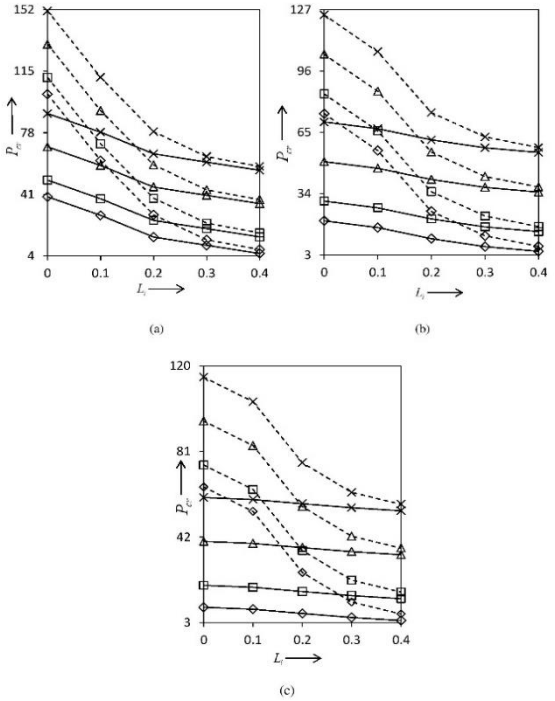

Fig. 7. Critical buckling load (a) C-C (b) C-S (c) S-S nanobeam for $K_w = 1$: —; $K_w = 1000$: ----; $K_g = 0(\diamond)$; $K_g = 10(\square)$; $K_g = 30(\triangle)$; $K_g = 50(\times)$

Figure 8 depicts a three-dimensional variation of critical buckling load for different values of the Winkler foundation parameter and nonlocal parameter keeping the shear foundation parameter constant for C-C, C-S, and S-S beams.

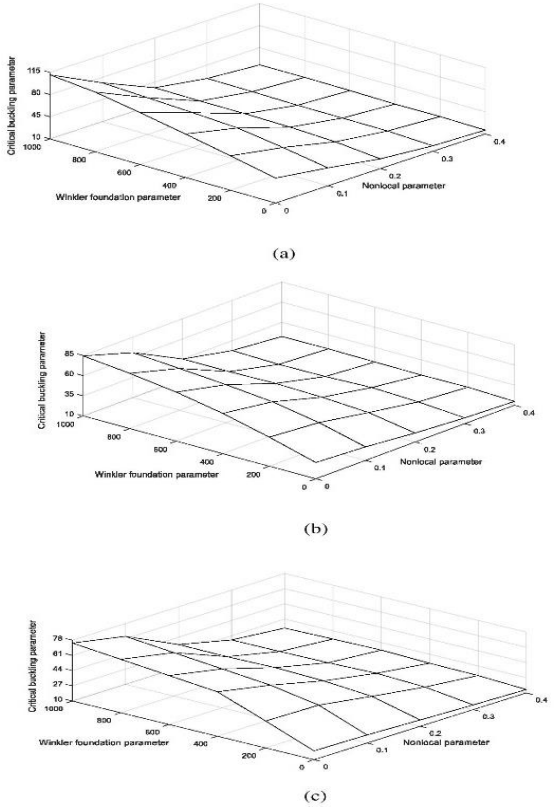

Fig. 8. Critical buckling load (a) C-C (b) C-S (c) S-S nanobeam for $K_g = 10$

Figure 9 presents a three-dimensional variation of critical buckling load for different values of shear foundation parameter and nonlocal parameter keeping the Winkler foundation parameter constant for C-C, C-S, and S-S beams.

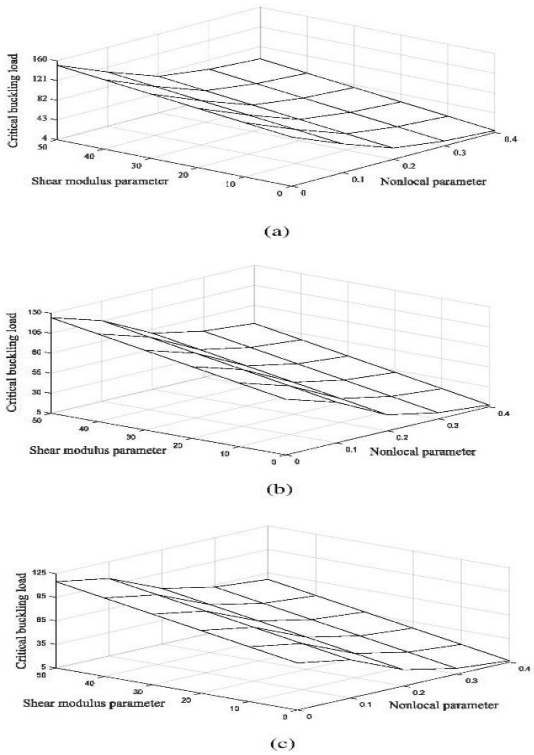

Fig. 9. Critical buckling load (a) C-C (b) C-S (c) S-S nanobeam for $K_w = 1000$

4. Conclusions

Free transverse vibration and buckling of an Euler-Bernoulli nanobeam resting on the Pasternak foundation have been studied on the basis of Eringen's nonlocal elasticity theory. The PDQM and the HDQM are used to obtain the first three values of the frequency parameter and the lowest critical buckling load. A computer program in C++ is developed to calculate the results. In this analysis, C-C, C-S, and S-S boundary conditions have been considered. The study shows that nonlocal parameters, boundary conditions, axial force parameters, and elastic foundation moduli have considerable impacts on the results. So, it is concluded from the present study that

(i) Frequencies decrease with an increase in nonlocal parameters except for frequency in the fundamental mode for C-C and C-S boundary conditions. The important observation is that for certain values of the Pasternak foundation parameter, the frequency in fundamental mode first increases and then decreases for C-C and C-S boundary conditions. The variation of

frequency with nonlocal parameter L_i is not monotonic in the first mode. In the second and third modes, frequency continuously decreases with an increase in the value of L_i.

(ii) The maximum frequency is observed for C-C boundary conditions followed by C-S and S-S boundary conditions, respectively.

(iii) The Winkler and the Pasternak foundation parameters have significant effects on the free vibration and stability behaviour of nanobeams. The critical buckling load increases with an increase in foundation moduli and decreases with an increase in the nonlocal parameter L_i.

(iv) The greatest buckling load is observed for C-C boundary conditions followed by C-S and S-S boundary conditions, respectively.

(v) The results obtained by the PDQM and the HDQM are identical.

Nomenclature

A	Cross-section area of the beam
C	Clamped edge
$C_{ij}{}^{(m)}$	Weighting coefficients of mth order
D	Flexural rigidity
E	Young's modulus of the plate material
I	Second moment of area
$K([x-x'],\alpha)$	Nonlocal modulus
K_w, K_g	Foundation parameters
k_w, k_g	Winkler and shear foundation stiffnesses
L	Length of the beam
M	Bending moment
N	Number of grid points
p	Compressive load
P_{cr}	Critical buckling load
S	Simply supported edge
t	Time
T	Kinetic energy of the beam
U	Strain energy of the beam
w	Transverse deflection
W	Non-dimensional transverse deflection
W_f	Potential energy due to Pasternak foundation
W_p	Work done by the compressive load
$\frac{e_0 a}{L}$	Nonlocal parameter
ω	Circular frequency
ρ	Density of beam material
σ_{xx}	Normal stress
ε_{xx}	Normal strain
Ω	Frequency parameter
∇^2	The Laplace operator

Algorithm of C++

Step 1: Generation of grid points

Step 2: Generation of weighting coefficients

Step 3: Discretization of governing equation at grid points

Step 4: Implementation of boundary conditions

Step 5: Implementation of bisection method to obtain frequencies and critical buckling loads.

Conflicts of Interest

The authors declare that there is no conflict of interest between the authors.

Acknowledgment

The authors are thankful to the learned reviewers for their critical comments to improve the quality of the paper.

References

[1] Iijima, S., 1991. Helical microtubules of graphitic carbon. *Nature*, 354, pp.56-58.

[2] Baughman, R.H., Zakhidov, A.A., De Heer, W.A., 2002. Carbon nanotubes--the route toward applications. *Science*, 297, pp.787-792.

[3] Wang, X., Cai, H., 2006. Effects of initial stress on non-coaxial resonance of multi-wall carbon nanotubes. *Acta Materialia*, 54(8), pp.2067-2074.

[4] Eringen, A.C., 1972. Linear theory of non-local elasticity and dispersion of plane waves. *International Journal of Engineering Science*, 10(5), pp.425-435.

[5] Eringen, A.C., 1972. Nonlocal polar elastic continua. *International Journal of Engineering Science,* 10 (1), pp.l-16.

[6] Eringen, A.C., Edelen, D.G.B., 1972. On nonlocal elasticity. *International Journal of Engineering Science,* 10(3), pp.233-248.

[7] Eringen, A.C., 1983. On differential equations of nonlocal elasticity and solutions of screw dislocation and surface waves. *Journal of Applied Physics*, 54(9), pp.4703-4710.

[8] Lu, P., Lee H., Lu C., Zhang P., 2006. Dynamic properties of flexural beams using a nonlocal elasticity model. *Journal of Applied Physics*, 99(7), pp.073510(1-9).

[9] Xu, M., 2006. Free transverse vibrations of nano-to-micron scale beams. *Proceedings of the Royal Society A: Mathematical, Physical*

and Engineering Sciences, 462(2074), pp.2977-2995.

[10] Wang, C., Zhang, Y., He, X., 2007. Vibration of nonlocal Timoshenko beams. *Nanotechnology*, 18(10), pp.105401(1-9).

[11] Challamel, N., Wang, C. M., 2008. The small length scale effect for a non-local cantilever beam: A paradox solved. *Nanotechnology*, 19(34), pp.345703(1-7).

[12] Murmu, T., Pradhan, S., 2009. Small-scale effect on the vibration of nonuniform nanocantilever based on nonlocal elasticity theory. *Physica E*, 41(8), pp.1451-1456.

[13] Roque, C., Ferreira, A., Reddy, J., 2011. Analysis of Timoshenko nanobeams with a nonlocal formulation and meshless method. *International Journal of Engineering*, 49(9), pp.976-984.

[14] Mohammadi, B., Ghannadpour, S., 2011. Energy approach vibration analysis of nonlocal Timoshenko beam theory. *Procedia Engineering*, 10, pp.1766-1771.

[15] Li, C., Lim, C.W., Yu, J.L., 2011. Dynamics and stability of transverse vibrations of nonlocal nanobeams with a variable axial load. *Smart Materials and Structures*, 20(1), pp.015023(1-7).

[16] Eltaher, M.A., Alshorbagy, A.E., Mahmoud, F.F., 2013. Vibration analysis of Euler-Bernoulli nanobeams by using finite element method. *Applied Mathematical Modelling*, 37, pp.4787-4797.

[17] Behera, L., Chakraverty, S., 2014. Free vibration of Euler and Timoshenko nanobeams using boundary characteristic orthogonal polynomials. *Applied Nanoscience*, 4(3), pp.347-358.

[18] Rahmani, O., Pedram, O., 2014. Analysis and modeling the size effect on vibration of functionally graded nanobeams based on nonlocal Timoshenko beam theory. *International Journal of Engineering Science*, 77, pp.55-70.

[19] Behera, L., Chakraverty, S., 2015. Application of Differential Quadrature method in free vibration analysis of nanobeams based on various nonlocal theories. *Computers & Mathematics with Applications*, 69(12), pp.1444-1462.

[20] Ebrahimi, F., Salari, E., 2015. Size-dependent free flexural vibrational behavior of functionally graded nanobeams using semi analytical differential transform method. *Composites Part B Engineering*, 79, pp.156-169.

[21] Ebrahimi, F., Ghadiri, M., Salari, E., Hoseini, S.A.H., Shaghaghi, G.R., 2015. Application of the differential transformation method for nonlocal vibration analysis of functionally graded nanobeams. *Journal of Mechanical Science and Technology*, 29(3), pp.1207-1215.

[22] Tuna, M., Kirca, M., 2016. Exact solution of Eringen's nonlocal integral model for vibration and buckling of Euler-Bernoulli beam. *International Journal of Engineering Science*, 107, pp.54-67.

[23] Hamza-Cherif, R., Meradjah, M., Zidour, M., Tounsi, A., Belmahi, S., Bensattalah, T., 2018. Vibration analysis of nano beam using differential transform method including thermal effect. *Journal of Nano Research*, 54, pp.1-14.

[24] Aria, A.I., Friswell, M.I., 2019. A nonlocal finite element model for buckling and vibration of functionally graded nanobeams. *Composites Part B*, 166, pp.233-246.

[25] Nikam, R.D., Sayyad, A.S., 2020. A unified nonlocal formulation for bending, buckling and free vibration analysis of nanobeams. *Mechanics of Advanced Materials and Structures*, 27(10), pp.807-815.

[26] Arian, B., Hamidreza, S., Nima, K., 2020. Effect of the thickness to length ratio on the frequency ratio of nanobeams and nanoplates. *Journal of Theoretical and Applied Mechanics*, 58(1), pp.87-96.

[27] Ufuk, G., 2022. Transverse free vibration of nanobeams with intermediate support using nonlocal strain gradient theory. *Journal of Structural Engineering & Applied Mechanics*, 5(2), pp.50-61.

[28] Wang, C.M., Zhang, Y.Y., Ramesh, S.S., Kitipornchai, S., 2006. Buckling analysis of micro and nano-rods/tubes based on nonlocal Timoshenko beam theory. *Journal of Physics D. Applied Physics*, 39, pp.3904-3909.

[29] Reddy, J.N., 2007. Nonlocal theories for bending, buckling and vibration of beams. *International Journal of Engineering Science*, 45, pp.288-307.

[30] Pradhan, S.C., Phadikar, J.K., 2009. Bending, buckling and vibration analyses of nonhomogeneous nanotubes using GDQ and nonlocal elasticity theory. *Structural Engineering and Mechanics*, 33(2), pp.193-213.

[31] Aydogdu, M., 2009. A general nonlocal beam theory: Its application to nanobeam bending,

buckling and vibration. *Physica E*, 41, pp.1651-1655.

[32] Thai, H.T., 2012. A non-local beam theory for bending, buckling, and vibration of nano beams. *International Journal of Engineering Science*, 52, pp.56-64.

[33] Eltaher, M. A., Emam S. A., Mahmoud F. F., 2013. Static and stability analysis of nonlocal functionally graded nanobeams. *Composite Structures*, 96, pp.82-88.

[34] Ebrahimi, F., Salari, E., 2015. A semi-analytical method for vibrational and buckling analysis of functionally graded nanobeams considering the physical neutral axis position. *Computer Modeling in Engineering & Sciences*, 105, pp.151-181.

[35] Nejad, M.Z., Hadi, A., Rastgoo, A., 2016. Buckling analysis of arbitrary two-directional functionally graded Euler-Bernoulli nano-beams based on nonlocal elasticity theory. *International Journal of Engineering Science*, 103, pp.1-10.

[36] Safarabadi, M., Mohammadi, M., Farajpour, A., Goodarzi, M., 2015. Effect of surface energy on the vibration analysis of rotating nanobeam. *Journal of Solid Mechanics*, 7 (3), pp. 299-311.

[37] Mohammadi, M., Safarabadi, M., Rastgoo, A., Farajpour, A., 2016. Hygro-mechanical vibration analysis of a rotating viscoelastic nanobeam embedded in a visco-Pasternak elastic medium and in a nonlinear thermal environment. *Acta Mechanica*, 227, pp. 2207-2232.

[38] Zhu, X., Wang, Y. and Dai, H.H., 2017. Buckling analysis of Euler–Bernoulli beams using Eringen's two-phase nonlocal model. International Journal of Engineering Science, 116, pp.130-140.

[39] Khaniki, H.B., Hosseini-Hashemi, S., 2017. Buckling analysis of tapered nanobeams using nonlocal strain gradient theory and a generalized differential quadrature method. *Materials Research Express*, 4(6), pp.065003.

[40] Tuna, M., Kirca, M., 2017. Bending, buckling and free vibration analysis of Euler–Bernoulli nanobeams using Eringen's nonlocal integral model via finite element method. *Composite Structures*, 179, pp.269-284.

[41] Bakhshi, K.H., Hosseini-Hashemi, S., Nezamabadi, A., 2018. Buckling analysis of nonuniform nonlocal strain gradient beams using generalized differential quadrature method. *Alexandria Engineering Journal*, 57, pp.1361-1368.

[42] Soltani, M., Mohammadi, M., 2018. Stability analysis of non-local Euler-Bernoulli beam with exponentially varying cross-section resting on Winkler-Pasternak foundation. *Numerical Methods in Civil Engineering*, 2(3), pp.1-11.

[43] Xu, X., Zheng, M., 2019. Analytical solutions for buckling of size-dependent Timoshenko beams. *Applied Mathematics and Mechanics*, 40, pp.953-976.

[44] Jena, S.K., Chakraverty, S., 2019. Differential quadrature and differential transformation methods in buckling analysis of nanobeams. *Curved Layer Structures*, 6, pp.68-76.

[45] Ragb, O., Mohamed, M., Matbuly, M.S., 2019. Free vibration of a piezoelectric nanobeam resting on nonlinear Winkler-Pasternak foundation by quadrature methods. *Heliyon*, 5(6), e01856.

[46] Nazmul, I.M., Devnath, I., 2021. Closed-form expressions for bending and buckling of functionally graded nanobeams by the Laplace transform. *International Journal of Computational Materials Science and Engineering*, 10(2), pp.2150012.

[47] Karmakar, S., Chakraverty, S., 2021. Differential quadrature and Adomian decomposition methods for solving thermal vibration of Euler nanobeam resting on Winkler-Pasternak foundation. *Journal of Mechanics of Materials and Structures*, 16 (4), pp.555-572.

[48] Zewei, L., Baichuan, L., Bo, C., Xiang, Z., Yinghui, L., 2022. Free vibration, buckling and dynamical stability of Timoshenko micro/nano-beam supported on Winkler-Pasternak foundation under a follower axial load. *International Journal of Structural Stability and Dynamics*, 22(09), pp.2250113

[49] Civalek, Ö., Uzun, B., Yaylı, M. Ö., 2022. An effective analytical method for buckling solutions of a restrained FGM nonlocal beam. *Computational & Applied Mathematics,* 41(2), pp.1-20.

[50] Jalaei, M.H., Thai, H-T., Civalek, Ö., 2022. On viscoelastic transient response of magnetically imperfect functionally graded nanobeams. *International Journal of Engineering Science*, 172, pp.103629.

[51] Beni, Y.T., 2022. Size dependent torsional electro-mechanical analysis of flexoelectric micro/nanotubes. *European Journal of Mechanics - A/Solids*, 95, pp.104648.

[52] Beni, Z.T., Beni, Y.T., 2022. Dynamic stability analysis of size-dependent viscoelastic/piezoelectric nano-beam. *International Journal of Structural Stability and Dynamics*, 22(5), pp.2250050.

[53] Numanoğlu, H.M., Ersoy, H., Akgöz, B., Civalek, Ö., 2022. A new eigenvalue problem solver for thermo-mechanical vibration of Timoshenko nanobeams by an innovative nonlocal finite element method. *Mathematical Methods in the Applied Sciences*, 45(5), pp. 2592-2614.

[54] Karmakar, S., Chakraverty, S., 2022. Thermal vibration of nonhomogeneous Euler nanobeam resting on Winkler foundation. *Engineering Analysis with Boundary Elements*, 140, pp.581-591.

[55] Abbas, W., Bakr, O.K., Nassar, M.M., Abdeen, M.A.M., Shabrawy, M., 2021. Analysis of tapered Timoshenko and Euler-Bernoulli beams on an elastic foundation with moving loads. *Journal of Mathematics*, https://doi.org/10.1155/2021/6616707.

[56] Wang, C.M., Reddy, J.N., Lee, K.H., 2000. *Shear deformable Beams and Plates: Relationships with classical solutions*. Elsevier.

[57] Murmu, T., Adhikari, S., 2010. Nonlocal transverse vibration of double-nanobeam-systems. *Journal of Applied Physics*, 108, pp.083514(1-9).

[58] Bert, C.W., Malik, M., 1996. Differential quadrature method in computational mechanics: A review. *Applied Mechanics Reviews*, 49(1), pp.1-28.

[59] Civalek, Ö., 2004. Application of differential quadrature (DQ) and harmonic differential quadrature (HDQ) for buckling analysis of thin isotropic plates and elastic columns. *Engineering Structures*, 26, pp.171-186.

[60] Shu, C., 2000. Differential quadrature and its application in engineering. Springer Science & Business Media.

[61] Demir, C., 2016. Nonlocal vibration analysis for micro/nano beam on Winkler foundation via DTM. *International Journal of Engineering and Applied Sciences*, 4, pp.108-118.

[62] Rahbar-Ranji, A., Shahbaztabar, A., 2017. Free vibration analysis of beams on a Pasternak foundation using Legendre polynomials and Rayleight-Ritz method. *Proceedings of Odessa Polytechnic University*, 3(53), pp.20-31.

[63] Ghannadpour, S.A.M., Mohammadi, B., Fazilati, J., 2013. Bending, buckling and vibration problems of nonlocal Euler beams using Ritz method. *Composite Structures*, 96, pp.584-589.

[64] Sari, M.E.S., Al-Kouz, W.G., Atieh, A., 2018. Buckling analysis of axially functionally graded tapered nanobeams resting on elastic foundations, based on nonlocal elasticity theory. *Strojniski Vestnik-Journal of Mechanical Engineering*, 64, pp.772-782.